Proceedings of the 2010 IEEE
International Conference on Robotics and Biomimetics
December 14-18, 2010, Tianjin, China

Ultra-miniaturized WB-3 Inertial Measurement Unit: performance evaluation of the attitude estimation

S. Sessa, *Member, IEEE,* M. Zecca, *Member, IEEE,* Z. Lin, *Student Member, IEEE*, L. Bartolomeo, *Student Member, IEEE,* K. Itoh, H. Ishii, Y. Mukaeda, Y. Suzuki, and A. Takanishi, *Member, IEEE*

***Abstract*— This paper presents the comparison of the WB-3 ultra-miniaturized inertial measurement unit (IMU), developed by our group, with the commercial IMU InertiaCube by InterSense and the Vicon motion capture system. WB-3 is provided with a 32-bit microcontroller and 9-axis inertial sensors (miniaturized MEMS accelerometer, gyroscope and magnetometer). We implemented an Extended Kalman Filter (EKF) based on quaternion for the sensor fusion to retrieve the attitude. A new methodology for the automatic estimation of the measurement covariance matrix on the EKF is presented (R-Adaptive Algorithm). The preliminary results showed that WB-3 performance is comparable with Vicon. The R-Adaptive Algorithm improves the attitude reconstruction in case of non-static condition compared with the commercial IMU.**

I. Introduction

IN the last years the interest on motion capture systems is increased in many application fields. Medical applications, for example, paid a growing attention to human motion caption systems to obtain more efficient rehabilitation therapies [1-2], and to build monitoring networks for patients and elder people in the hospitals and in their own homes [3-5]. In game industry, the market trend is toward active game platforms, where a smart wearable motion capture suite could expand the capability of this kind of games and open total virtual reality scenarios, at the edge of the augmented reality. Moreover, distributed sensors architectures for motion capture would be hosted on different structure of robots, like manipulators and rovers. Industrial manipulators, small smart arms and, in general, exoskeleton parts with these sensors and cognition capability should help people to avoid any physical risk in object manipulation and environment interaction.

Although several motion capture technologies have been developed in the past years, such as optical, image-based [6], mechanical [7], magnetic, and acoustic [8], these methods do not cover all the application fields discussed above.

For example, optical motion capture systems are preferred in the computer-animation community, in the film industry and medical contexts [9-10], because they offer a reliable and accurate way to record the motions of complex systems; however, this approach is expensive and poor in portability. In fact, these systems use 3D markers, such as light-emitting diodes or passive reflectors, placed on the body. They compute the exact locations of the markers from the images recorded by the surrounding cameras using triangulation methods; therefore, they can be used only in a structured environment [11].

A very promising frontier on the wearable and reliable MOtion CAPture system (MOCAP) is based on Inertial Measurement Unit (IMU) which can be virtually used everywhere.

This paper presents the comparison of the WB-3 Ultra-miniaturized IMU, developed by our group, with the commercial IMU InertiaCube by InterSense and the Vicon motion capture system. In the commercial IMUs often there are problems on the correction of the pitch and roll angles by using the accelerometer; due to the strong hypothesis of negligible linear accelerations in respect to the gravity. To overcome this limitation, a new methodology for the estimation of the measurement covariance matrix (R-Adaptative Algorithm) in the quaternion based Extended Kalman Filter (EKF) is presented.

Section II of the paper describes the WB-3 device and the Experimental setup for the performance evaluation of the IMU. Section III describes the structure of the implemented EKF for the attitude calculation. The EKF is based on the

Manuscript received July 23, 2010. This research has been partially supported by a Grant by STMicroelectronics, which also provided the core sensors and the microcontroller. This work was also supported in part by Global COE Program "Global Robot Academia", MEXT, Japan; the Advancement of University Education Project of Chinese government Grant # [2007] – 3020; the JSPS Grant-in-aid for Scientific Research #19700389; the Waseda University Grant for Special Research Projects (No. 266740); and the JSPS Postdoctoral Fellowship Program for Foreigner Researcher FY2008. The authors would like to express their thanks to the Italian Ministry of Foreign Affairs, General Directorate for Cultural Promotion and Cooperation, for its support to RoboCasa. The authors would also like to express their gratitude to Okino Industries LTD, Japan ROBOTECH LTD, SolidWorks Corp, Dyden, for their support to the research.

S. Sessa, is with Graduate School of Advanced Science and Engineering , Waseda University, 2-2 Wakamatsu-cho, Shinjuku-ku,Tokyo 168-8480, Japan (salvatore@takanishi.mech.waseda.ac.jp)

M. Zecca is with the School of Creative Science and Engineering, Faculty of Science and Engineering, Waseda University, Tokyo, Japan (zecca@aoni.waseda.jp). He is also a member of the Humanoid Robotics Institute (HRI) and of the Italy-Japan Joint Laboratory on Humanoid and Personal Robotics "RoboCasa".

Z. Lin, L. Bartolomeo and H. Ishii are with the Global Robot Academia, Waseda University, 3-4-1 Okubo, Shinjuku-ku, Tokyo, 169-8555, Japan (Z. Lin: zhuohualin@ruri.waseda.ac.jp).

K. Itoh is with the Advanced Research Institute for Science and Engineering, and the Italy-Japan Joint Laboratory on Humanoid and Personal Robotics "RoboCasa", Waseda University, Japan.

Y. Mukaeda, and Y. Suzuki are with Graduate School of Advanced Science and Engineering Waseda University.

A. Takanishi is with the Department of Modern Mechanical Engineering, Waseda University, Tokyo, Japan (takanisi@waseda.jp). He is also one of the core members of the Humanoid Robotics Institute (HRI) and of the Italy-Japan Joint Laboratory on Humanoid and Personal Robotics "RoboCasa".

978-1-4244-9318-0/10/$26.00 © 2010 IEEE

quaternion representation to determinate the IMU attitude using the information of the accelerometer and gyroscope sensors. Furthermore, on this section the techniques of data synchronization among the different measurement systems used in the experiments are described.

Eventually, the experimental protocol and the results of the comparison on the attitude estimation using WB-3, InertiaCube and Vicon are presented on the section IV.

II. Material and Methods

A. Inertial Measurement Unit IMU WB-3

Our group has recently developed a new IMU very compact and lightweight (size 20 x 20 mm and weight 2.9 g). A picture of the WB-3 IMU is shown in Fig. 1. The IMU is composed by the following sensors: 3-axis Accelerometer LIS3LV02DL; 2-axis gyroscope IDG300; 1-axis gyroscope LSIY300AL. The IMU also includes a 3-axis Magnetometer HMC5843; however the data of this sensor have not been analyzed for this paper, and therefore its description is omitted. The characteristics of the WB-3 sensors are summarized in TABLE I.

The LIS3LV02DL (STMicroelectronics) is a 3-axis accelerometer, whose small size (4.4 x 7.5 x 1 mm) and high performance characteristics are fully compatible with the requirements of the human motion analysis. The resolution with a Full-scale ±2 G and Bandwidth of 160 Hz is 2 mG, with noise level of about 0.005 m/sec^2, less than one bit. The LISY300AL (STMicroelectronics) is a miniaturized 7.0x7.0x1.9 mm z-axis gyro sensor. Its full-scale is ±300 deg/s with a Bandwidth of 88 Hz and a sensitivity of 3.3 mV/deg/s. In order to measure 3-axial angular rates, we also used a bi-axial gyro IDG300 (InvenSense). The IDG300 size is 6.0×6.0×1.5 mm, the measurement range is ±500 deg/s and the sensitivity is 2.0 mV/deg/s. This mixed configuration allows our IMU to obtain all the 3 axis of the gyros in one planar layer.

WB-3 IMU contains a STMicroelectronics 32-bit microcontroller STM32 Cortex for embedded signal elaboration and data transmission. The communication with the module is performed using a CAN BUS at 1Mb/s, directly connected with a PC. The block diagram of the WB-3 Inertial Measurement Unit is showed in Fig. 2 and a detailed description of the architecure is on [12]. The WB-3 has already been successfully applied for the analysis of the human body movements in medical application [12-13].

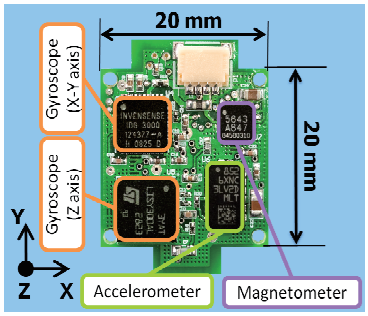

Fig. 1. WB-3 Inertial Measurement Unit

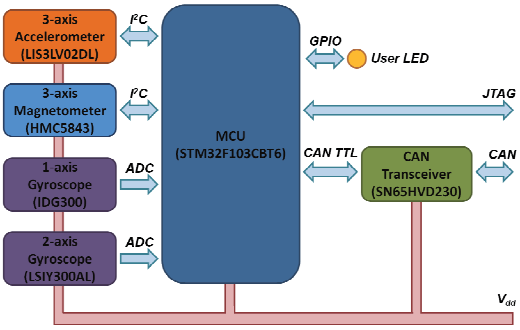

Fig. 2. Block diagram of WB-3

TABLE I
Main characteristics of the WB-3 sensors

	LIS3LV02DL	IDG300	LSIY300AL
Range	±2 G	±500 deg/s	±300 deg/s
Sensitivity	12±1 bit	12±1 bit	12±1 bit
Bandwidth	40 Hz	140 Hz	88 Hz
Linearity (FS)	±2%	<1%	±0.8%
Noise level	0.0051 m/s^2	0.35 deg/s	0.26 deg/s

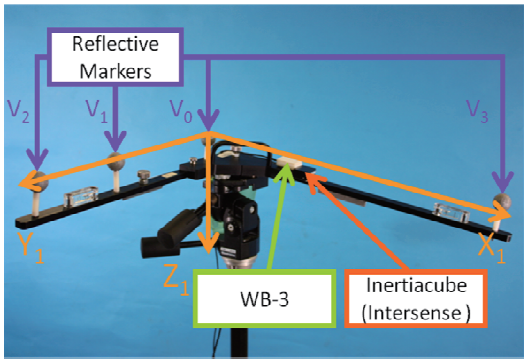

Fig. 3. Experimental setup: L-frame with reflective markers, InertiaCube and WB-3

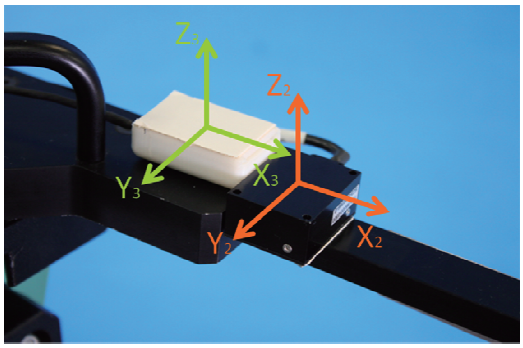

Fig. 4. WB-3 and InertiaCuber

B. Experimental setup

The evaluation of the implemented EKF algorithm was performed using the WB-3 platform compared with a commercial IMU (InertiaCube by Intersense) [14] and the Vicon system [11].

To construct the data set for the analysis, the WB-3 platform and the commercial IMU were linked with a metallic L-frame using adhesive as shown in Fig. 3. The metallic L-frame has four reflective markers in order to determine its exact attitude in the global Vicon reference system. For the first experiment, the system was moved around the y-axis of the L-frame at different speeds (X_1-Y_1-Z_1). Additionally, in the second experiment the L-frame was moved freely on the space at different speeds.

During these movements (total execution time 150 s) the orientation data were computed by the WB-3, InertiaCube and the Vicon. All the data were logged and off-line compared.

III. WB-3 DATA FUSION ALGORITHM

A. EKF for attitude estimation

The idea behind the sensor fusion is that, using several kinds of sensors, the characteristics of one type of sensor avoid overcoming the limitation of other sensors.

In this way, the Kalman filter is useful for combining data from several different noisy measurements. In fact, gyroscopes measure orientation by integrating angular rates and the accelerometer and magnetometer provide a noisy and disturbed but drift-free measurement of orientation. The Kalman filter weights the three sources of information appropriately with knowledge about the signal characteristics based on their models, to make the best use of all sensor data [15].

In general, the Extended Kalman Filter algorithm addresses the problem of trying to estimate the state of a discrete-time process described by the equations below [16]:

$$x_{k+1} = A_k x_k + B_k u_k + w_k \tag{1}$$

$$z_k = H_k x_k + v_k \tag{2}$$

where x is the state vector; u is the input vector; A_k, B_k, H_k, are respectively state, input, and output matrix; w, v are state and measurement noise. The state and measurement noise are Gaussian and white noise sources with covariance matrix Q and R respectively.

At each time step, the algorithm propagates both the state estimation and the error covariance matrix. The latter provides an indication of the uncertainty associated with the current state estimation. These are evaluated in the prediction equations.

The Kalman Gain is derived from minimizing the a posteriori error covariance, and it could be considered as a measurement of the level of confidence to give to the predict state.

B. Quaternion Based EKF

In the IMUs, the main problem is that the orientation is computed by the integration of the gyro signals including any superimposed sensor drift and noise. The orientation drift errors, resulting from gyro output errors, can be bounded by additional sensors (in this case the 3-axis accelerometer), whose information allow correcting the orientation drift. In this way the earth's gravitational field vectors is resolved by the aiding system in the body frame, with their known representation in the absolute reference frame [16]. In the present work, a classic state augmentation technique is applied in the process model, and the state vector is composed by orientation and gyro bias. Quaternions are used to represent space orientation to improve computational efficiency and avoid singularities [17]. After EKF running, the computed quaternions could be translated into Roll, Pitch and Yaw angles, through transformation equations [16].

The continuous-time, non linear system equations are[15]:

$$\dot{x} = f(x, \omega) + w \tag{3}$$

$$y = h(x) + v \tag{4}$$

where $x = [q\ b_\omega]^T$ represents the state of the system composed by the quaternion $q = [q_0\, q_1\, q_2\, q_3]$ and the rate gyro bias $b_\omega = [b_{\omega x}\, b_{\omega y}\, b_{\omega z}]$; ω is the angular rates vector $[\omega_x\, \omega_y\, \omega_z]$; $y = a$ is the measurement vector composed by the acceleration measurements $[a_x\, a_y\, a_z]$.

In a strap-down inertial navigation system, the rigid body angular motion is described by the differential equation

$$\dot{q} = \begin{bmatrix} [\vec{\omega}\times] & \vec{\omega} \\ -\vec{\omega}^T & 0 \end{bmatrix} q \tag{5}$$

where

$$[\vec{\omega}\times] = \begin{bmatrix} 0 & -\omega_z & \omega_y \\ \omega_z & 0 & -\omega_x \\ -\omega_y & \omega_x & 0 \end{bmatrix} \tag{6}$$

with the assumption that $||q|| = 1$.

Using the sensor model described in [14], in quasi static condition, the acceleration acting on the body is negligible compared to the gravity acceleration as described by:

$$\begin{cases} \vec{\omega} = G_g \omega_r + \vec{b}_\omega + \vec{v}_g \\ \vec{a} = G_a \left[C_n^b(q)(\vec{g}) \right] + \vec{v}_a \end{cases} \tag{7}$$

where G_g, G_a are respectively gyroscope and accelerometer gain, supposed constant; v_g, v_a are respectively gyroscope and accelerometer noise; ω is the gyroscope raw data; $C_n^b(q)$ is the direction cosine matrix in terms of orientation quaternion, that represents the coordinate transformation from the absolute coordinate systems n to the sensor frame b:

$$C_n^b(q) = \begin{bmatrix} q_1^2 - q_2^2 - q_3^2 + q_4^2 & 2(q_1 q_2 + q_3 q_4) & 2(q_1 q_3 - q_2 q_4) \\ 2(q_1 q_2 - q_3 q_4) & -q_1^2 + q_2^2 - q_3^2 + q_4^2 & 2(q_2 q_3 + q_1 q_4) \\ 2(q_1 q_3 + q_2 q_4) & 2(q_2 q_3 - q_1 q_4) & -q_1^2 - q_2^2 + q_3^2 + q_4^2 \end{bmatrix} \tag{8}$$

and $\vec{g} = [0\ 0\ -g]^T$ is the gravity vector in the base frame.

The non-linear functions, $f(x, \omega)$, and $h(x)$ in 3 and 4 can be explained as:

$$f(x, \omega) = \begin{bmatrix} \frac{1}{2} \begin{bmatrix} -q_1 & -q_2 & -q_3 \\ q_0 & -q_3 & q_2 \\ q_3 & q_0 & -q_1 \\ -q_2 & q_1 & q_0 \end{bmatrix} \begin{bmatrix} \omega_x - b_{\omega x} \\ \omega_y - b_{\omega y} \\ \omega_z - b_{\omega z} \end{bmatrix} \\ 0^{3x1} \end{bmatrix} \tag{9}$$

$$h(x) = C_n^b(q)\vec{g} \tag{10}$$

Because of its non-linearity, the system is linearized by calculating the Jacobian of f and h functions, therefore an EKF is implemented.

The estimation step of the EKF uses the angular rate to make a prediction of the state. Furthermore, the acceleration data are used to correct Roll and Pitch angles in the "Roll-Pitch Update" block as showed in the Fig. 5. The correction of the yaw angle "Yaw Update" can be performed using the magnetometer (Magnetic North). The focus of this paper is the "Roll-Pitch Update" block (dark part of the block diagram in Fig. 5); the problems and limitations of the

magnetic correction in the EKF were addressed from several researchers in [18-21].

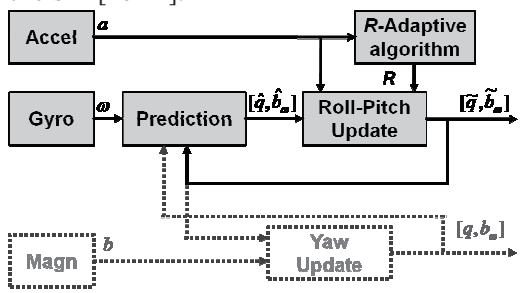

Fig. 5. Block diagram of the EKF algorithm implemented for WB-3

C. R-Adaptive algorithm

The main limitation of the algorithm described in the previous section is related to the "quasi-static condition", in which the linear accelerations are negligible compared to the gravity acceleration. In the case of human motion tracking (i.e. during walking or running), often this condition is not verified.

To overcome the problems related to the correction of the attitude using the data from the accelerometer, several techniques have been previously used [22]. Some techniques check the angular rate and the module of acceleration to determine quasi-static conditions. If a quasi-static condition is detected, the Update phase of the EKF is performed, otherwise it is just skipped. These techniques solve quite efficiently the drawback of the EKF, however the threshold that discriminates between the dynamic and static conditions must be chosen opportunely. Furthermore, it is difficult to set the coefficients of the measurement covariance matrix (R). Not only the measurement noise, but also the error due to the linear accelerations should be considered for a correct evaluation. To overcome these problems, the R-adaptive algorithm has been implemented.

R is assumed to be in this form:

$$R = \begin{bmatrix} \sigma_x^2 & 0 & 0 \\ 0 & \sigma_y^2 & 0 \\ 0 & 0 & \sigma_z^2 \end{bmatrix} \tag{11}$$

where σ_x, σ_y, and σ_z are the standard deviations of the measurements respectively for the x, y and z axis of the acceleration sensors.

Considering the sensors axis with the same noise characteristics ($\sigma_x = \sigma_y = \sigma_z = \sigma$), it is possible to model the standard deviation as:

$$\sigma = \sigma_0 + \sigma_d \tag{12}$$

where σ_0 is the standard deviation in static condition, due to the accelerometer noise; σ_d is the standard deviation due to acceleration of the body, that deviates from static conditions. σ can be estimated in a temporal window with the following formula:

$$\sigma_k^2 = \frac{1}{N+1}\sum_{k=-N}^{k}\left(\|a_k\| - \|a_{k-1}\|\right)^2 \tag{13}$$

where N is the number of samples of the temporal window; σ_k^2 is the estimated variance at step k; and $||a_k||$ is the module of the acceleration measured by the accelerometer at the step k.

D. Data synchronization

The WB-3 and Vicon system have a sample rate of 100 Hz which is enough for the majority of the applications in the human body movement analysis. The commercial IMU (InertiaCube) samples internally the sensors at 100 Hz but the sample rate of the attitude angle given by the sensor is quite variable with a main sample frequency of about 37 Hz (every 27 ms). As shown in Fig. 6 the Sample rate for the WB-3 is very stable, 99.98% of the samples were transmitted with a sample time of 10 ms. Conversely, InertiaCube transmits only 77% of the data every 27 ms, and a significant percentage of the data (more than 12%) were sent with a sampling rate over 80 ms. For an effective comparison with the other systems the data of the InertiaCube has been over-sampled in post-elaboration at the frequency of 100 Hz.

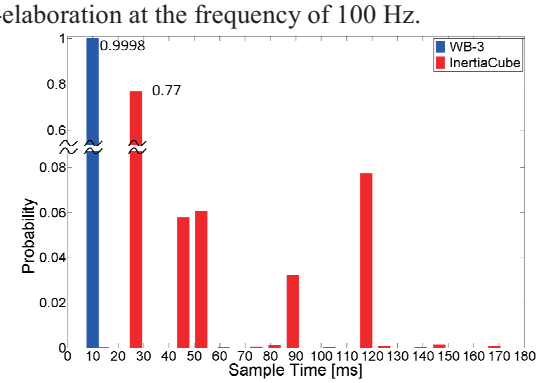

Fig. 6. Histogram of the Sample Time WB-3 (blue) and InertiaCube (red)

An important phase for the performance comparison of WB-3 with the other systems is the data synchronization. The Euclidean distance is an efficient distance measurement that can be used to determine similarity between time series (in our case the attitude measurements).

The Euclidian distance between two time series is simply the sum of the squared distances from each nth point in one time series to the nth point in the other. The main disadvantage of using Euclidean distance for time series data is that its results are very unintuitive. If two time series are identical, but one is shifted slightly along the time axis due to a no-perfect synchronization or variation of the sampling time, then Euclidean distance may consider them to be very different from each other.

To overcome this limitation and give intuitive distance measurements between time series, the Dynamic Time Warping (DTW) algorithm was introduced [23]; this algorithm scales the time dimension reducing the problems of both global and local shifts in the time. The result of the DTW on the data obtained from the WB-3 is shown in Fig. 7.

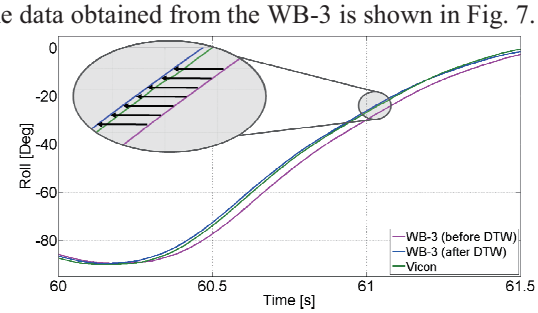

Fig. 7. DTW elaboration: WB-3 before DTW algorithm (magenta) WB-3 after DTW algorithm (blue) and Vicon (green)

IV. Experimental Validation

We validated the performance of WB-3 in two experiments:

- *Experiment a)* 45 rotations around the y-axis (Roll) at different speeds, for a total of 100 seconds of continuous acquisition;
- *Experiment b)* free rotations for a total of 50 seconds of continuous acquisitions.

The resulting average RMS errors for the Roll and Pitch are presented, for a) and b), in Table II and III respectively. Both WB-3 and InertiaCube follow quite well the trajectory. InertiaCube has an average RMS error of 2.2640 deg for the Roll movement, and 0.9183 deg for the Pitch in case of experiment a), 2.0767 deg and 5.9279 deg respectively for the Roll and Pitch in case of experiment b). Conversely, WB-3 has an average RMS error of 1.2337 deg, lower than InertiaCube, for the Roll movement, and 1.0739 deg, slighter higher than InertiaCube, for the Pitch in case of experiment a). For the experiment b) WB-3 has an average RMS error of 2.5474 deg and 1.0674 deg, respectively for the Roll and Pitch, about half of the error in the InertiaCube.

Fig. 8 (up) shows the reconstructed Roll angle for the *experiment a)*, the Fig. 8 (down) shows a detail of a single rotation. Fig. 9 shows the correspondent errors of WB-3 and InertiaCube compared to the Vicon system, for the Roll and Pitch. The results give evidence of better performance of WB-3, in particular for the Pitch movement as indicated in Table II.

Fig. 10. is a portion of the *experiment b)* where is shown the reconstructed angles (Roll and Pitch); and Fig. 11 shows the error comparison for the same time segment. The InertiaCube reconstructed angles show spikes during the rotations, because of linear accelerations applied to the sensor. The R-Adaptative Algorithm implemented on WB-3 is able to compensate the linear accelerations and reconstruct the angles with higher accuracy. It is also important to notice that, the attitude reconstruction algorithm of InertiaCube does not work if the pitch angle is around 90 deg because of singularity problems due to the Euler angle representations. The WB-3 algorithm is not affected by this problem because of the quaternion angle representation.

TABLE II

Experiment a) 100 sec - 45 rotation from 0 to 90° (x axis)

	RMS Roll Error [Deg]	RMS Pitch Error [Deg]
InertiaCube	2.2640	0.9183
WB-3	1.2337	1.0739

TABLE III

Experiment b) 50 sec - Free rotations

	RMS Roll Error [Deg]	RMS Pitch Error [Deg]
InertiaCube	2.0767	5.9279
WB-3	1.0674	2.5474

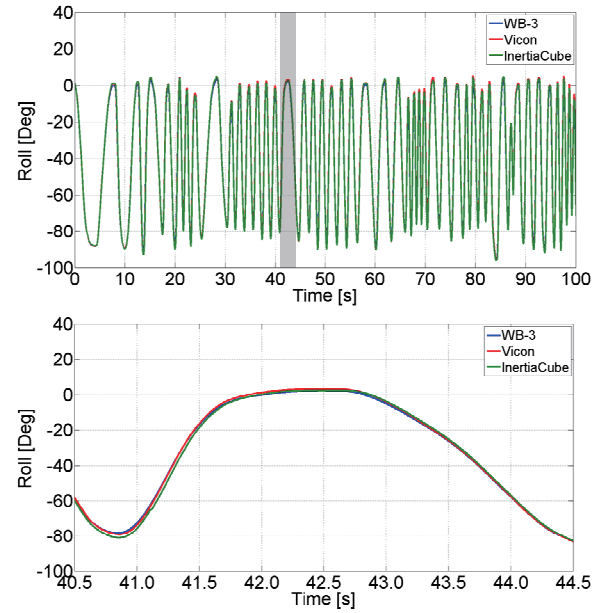

Fig. 8. *Experiment a)* Comparison of WB-3 and InertiaCube with Vicon during a 90 deg, Roll (up) Zoom of the gray area (down)

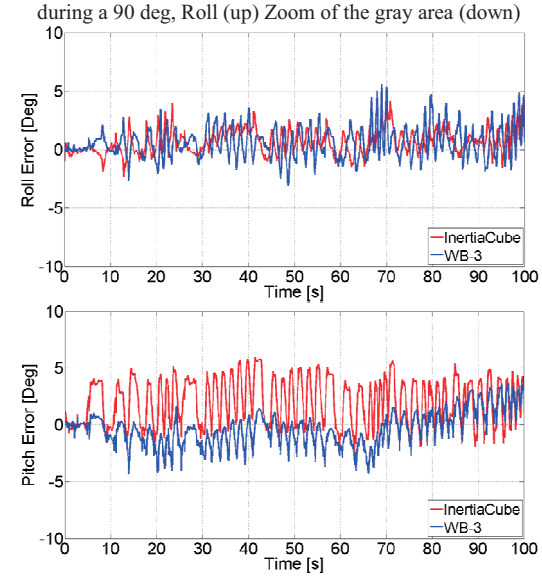

Fig. 9. Experiment a) Error comparison of WB-3 and InertiaCube with Vicon during a 90 deg, Roll (up) Pitch (down)

V. Conclusions

In this paper the WB-3 IMU has been presented (section II). The WB-3 module is provided with a microcontroller and 9-axis inertial sensors (miniaturized MEMS accelerometer, gyroscope and magnetometer), enabling it to retrieve the Roll, Pitch and Yaw angles by using an EKF for the sensor fusion (section III). The attitude obtained with WB-3 were compared with the attitude obtained with a commercial IMU (InertiaCube by Intersense) and the Vicon motion capture system. Preliminary results (section V) showed that the performances of WB-3 are comparable with the ones of Vicon. The advantage of WB-3 is the possibility to measure the human body movements, not only in a structured environment but virtually everywhere.

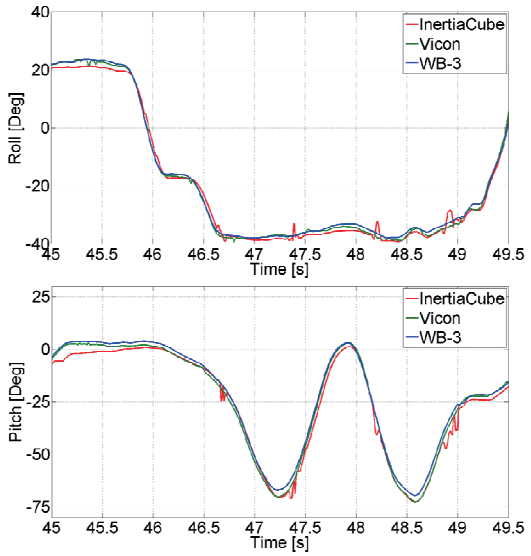

Fig. 10. Experiment b) Comparison of WB-3 and InertiaCube with Vicon free movements, Roll (up) Pitch (down)

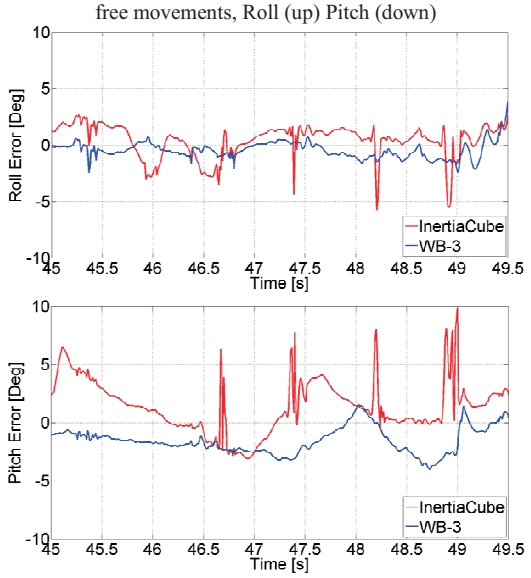

Fig. 11. Experiment b) Error comparison of WB-3 and InertiaCube with Vicon during free movements, Roll (up) Pitch (down)

Moreover, the implementation of the R-Adaptive algorithm allows the WB-3 to achieve better performance than the InertiaCube, especially when the hypothesis of negligible linear accelerations in respect to the gravity is not verified. The proposed IMU thanks to its performance, size, and weight, could be easily embedded in a tracksuit for total body motion reconstruction.

REFERENCES

[1] Y. Masuda, *et al.*, "An unconstrained monitoring system for home rehabilitation. A wireless heart/respiratory rate sensor accessible to home-visit therapists," *IEEE Eng Med Biol Mag,* vol. 24, pp. 43-47, Jul-Aug 2005.

[2] P. J. Bartosz, *et al.*, "Ubiquitous Rehabilitation Center: An Implementation of a Wireless Sensor Network Based Rehabilitation Management System," in *International Conference on Convergence Information Technology*, 2007, pp. 2349-2358.

[3] H. Lee, *et al.*, "A 24-hour health monitoring system in a smart house," *Gerontechnology,* vol. 7, pp. 22-35, 2008.

[4] B. Sachin, *et al.*, "Ubiquitous Healthcare Data Analysis and Monitoring Using Multiple Wireless Sensors for Elderly Person," *Sensor & Transducer Journal,* vol. 90, pp. 87-99, 2008.

[5] J. Orendurrff, *et al.*, "How humans walk: bout duration, steps per bout, and rest duration," *Journal of Rehabilitation Research & Development,* vol. 45, pp. 1077-1090, 2008.

[6] Y. Chen, *et al.*, "Markerless Monocular Motion Capture Using Image Features and Physical constraints," in *Computer Graphics International*, 2005, pp. 36-46.

[7] M. Zecca, *et al.*, "Analysis of the Surgeon's Performance during Laparoscopy by Using the Bioinstrumentation System WB-1R– towards the development of a Global Performance Index -," in *IEEE/RSJ International Conference on Intelligent Robots and Systems (IROS2007)*, Sheraton Hotel, San Diego, CA, USA, 2007, pp. 1272-1277.

[8] D. Vlasic, *et al.*, "Practical motion capture in everyday surroundings," *ACM Transactions on Graphics (TOG),* vol. 26, 2007.

[9] G. Venture, *et al.*, "Identification of human Limb Viscoelasticy using Robotics Methods to support the Diagnosys of Neuromuscular Diseases," *The International Journal of Robotics Research,* vol. 28, pp. 1322-1333, 2009.

[10] Y. Nakamura, *et al.*, "Somatosensory Computation for man-machine interface from motion-capture data and musculoskeletal human model," *IEEE Transations on Robotics,* vol. 21, pp. 58-66, 2009.

[11] Vicon Systems. (2009, *Vicon*. Available: http://www.vivometrics.com/

[12] M. Zecca, *et al.*, "Development of an Ultra-Miniaturized Inertial Measurement Unit for Objective Skill Analysis and Assessment in Neurosurgery: preliminary results," in *12th International Conference on Medical Image Computing and Computer Assisted Intervention MICCAI 2009*, Imperial College, London, 2009.

[13] Z. Lin, *et al.*, "Developement of an Ultra-Miniaturized Inertial Measurement Unit for Jaw Movement Analysis during Free Chewing," *Journal of Computer Science,* vol. 6, pp. 896-903, 2010.

[14] InterSense. (2010, *InertiaCube3*. Available: http://www.intersense.com

[15] R. E. Kalman, "A new Approach to Linear Filtering and Prediction Problems," *Transaction of the ASME-Journal of Basic Engineering,* pp. pp35-45, 1960.

[16] G. Bishop and G. Welch, "An Introduction to the Kalman Filter," presented at the SIGGRAPH course notes, 2001.

[17] A. M. Sabatini, "Quaternion-based extended Kalman filter for determining orientation by inertial and magnetic sensing," *IEEE Trans Biomed Eng,* vol. 53, pp. 1346-56, Jul 2006.

[18] R. Alonso and M. D. Shuster, "Attitude-Independent Magnetometer Bias Determination: A Survey," *Journal of the Astronautical Sciences,* vol. 50, pp. 453-475, 2002.

[19] D. Gebre-Egziabher, *et al.*, "A Non-Linear, Two-Step Estimation Algorithm for Calibrating Solid-State Strapdown Magnetometers," presented at the 8th International St. Petersburg Conference on Navigation Systems (IEEE/AIAA), St. Petersburg, Russia, 2001.

[20] D. Gebre-Egziabher, *et al.*, "Calibration of Strapdown magnetometers in Magnetic Field Domain," *Journal of Aerospace Engineering,* pp. 87-101, 2006.

[21] D. Campolo, *et al.*, "A novel procedure for In-field Calibration of Sourceless Inertial/Magnetic Orientation Tracking Wearable Devices," in *1st IEEE/RAS-EMBS International Conference on Biomedical Robotics and Biomechatronics (BioRob 2006)*, 2006.

[22] J. J. Kavanagh and H. B. Menz, "Accelerometry: A technique for quantifying movement patterns during walking," *Gait & Posture,* vol. 28, pp. 1-15, 2008.

[23] J. Kruskall and M. Liberman, *The Symmetric Time Warping Problem: From Continuous to DiscreteIn Time Warps, String Edits and Macromolecules: The Theory and Practice of Sequence Comparison,*. Massachusetts: Addison-Wesley Publishing Co., Reading, 1983